



Published in final edited form as:

Angew Chem Int Ed Engl. 2022 January 26; 61(5): e202110519. doi:10.1002/anie.202110519.

Directed Evolution of Artificial Metalloenzymes in Whole Cells

Dr. Yang Gu^{a,b,e}, Dr. Brandon J. Bloomer^{a,b}, Zhennan Liu^{a,b}, Reichi Chen^{a,b}, Douglas S. Clark^{c,d} [Prof.], John F. Hartwig^{a,b} [Prof.]

^aDepartment of Chemistry, University of California, Berkeley, California 94720, United States.

^bChemical Sciences Division, Lawrence Berkeley National Laboratory, 1 Cyclotron Road, Berkeley, California 94720, United States.

^cDepartment of Chemical and Biomolecular Engineering, University of California, Berkeley, California 94720, United States.

^dMolecular Biophysics and Integrated Bioimaging Division, Lawrence Berkeley National Laboratory, 1 Cyclotron Road, Berkeley, California 94720, United States.

^e**Present Address:** CAS Key Laboratory of Quantitative Engineering Biology, Shenzhen Institute of Synthetic Biology, Shenzhen Institutes of Advanced Technology, Chinese Academy of Sciences, Shenzhen, China

Abstract

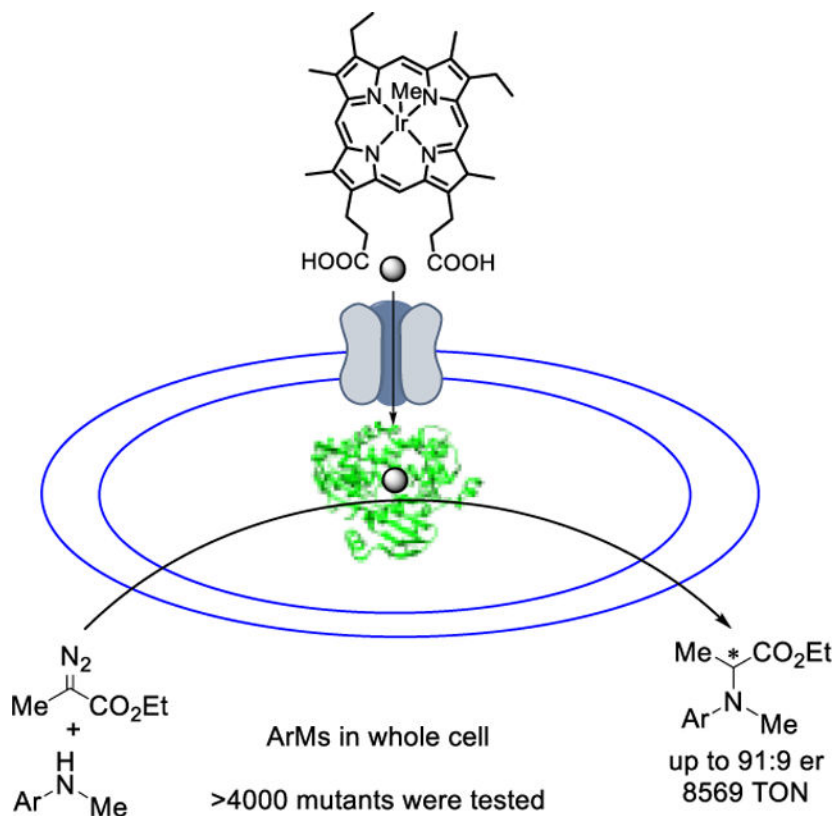
Artificial metalloenzymes (ArMs), created by introducing synthetic cofactors into protein scaffolds, are an emerging class of biocatalyst for non-natural reactions. In vitro reconstitution of cofactors and proteins has been a limiting step in the directed evolution of ArMs because purification of individual host proteins is time-consuming. We describe the application of a platform to combine the P450 enzyme and the cofactor Ir(Me)MPIX in vivo, with coexpression P450 and the heme transporter encoded by the *hug* operon. We applied this platform to the development an ArMs catalyzing the insertion of the acyclic carbene from α -diazopropanoate esters (Me-EDA) into the N-H bonds of N-alkyl anilines. The mutants of the ArMs Ir(Me)CYP119 identified by an evolution campaign involving more than 4000 mutants are shown to catalyze the reaction of Me-EDA with N-methyl anilines to form chiral amino esters with high TON and good enantioselectivity, there by demonstrating that the directed evolution of ArMs can rival that of natural enzymes in vivo.

Graphical Abstract

Whole-cell, *E. coli* platform enables directed evolution campaigns with ArMs containing an abiotic Ir-porphyrin cofactor involving the generation of more than 4000 mutants to develop an enantioselective insertion of a simple acyclic carbene from a diazo ester into the N-H bond of *N*-methyl aniline that has evaded prior enzyme systems and formed racemic product with mutants of natural P450s

jhartwig@berkeley.edu .

Supporting information for this article is given via a link at the end of the document.



Keywords

Artificial metalloenzymes; Directed evolution; Whole cell; N-H insertion; P450

Introduction

Enzymes are well-established catalysts for the selective and environmentally benign synthesis of fine chemicals and complex drugs.^[1] Although valuable, natural enzymes suffer from a limited scope of substrates and a limited set of transformations. Therefore, directed evolution and protein engineering has sought to expand the scope of unnatural substrates that react with natural enzymes and to achieve unnatural reactions for the construction of bioactive molecules. Examples range from the synthesis of sitagliptin catalyzed by an evolved transaminase^[2] to the transfer of carbenes catalyzed by repurposed hemoproteins.^[3]

The creation of artificial metalloenzymes (ArMs) possessing synthetic cofactors is a promising alternative strategy to achieve new reactivity with protein scaffolds. Strategies to create ArMs include the use of supramolecular assembly,^[4] anchoring of a cofactor to unnatural amino acids,^[5] and swapping native metals with noble metals.^[6] Like that of native enzymes for unnatural reactions, high reactivity and selectivity for reactions catalyzed by ArMs require modifications to the protein scaffold. The identification of appropriate modifications by directed evolution is often a slower process than with native classes of

enzymes, due to the additional step needed to introduce the abiotic cofactor and, in some cases, to remove the excess free cofactor.^[7]

Although screening for catalytic activity and selectivity in cell lysates can be faster than screening purified proteins, the construction of ArMs in cell lysates remains challenging, due to non-specific binding and inhibition caused by cytosolic compounds, such as glutathione (Figure 1, a).^[8] One could imagine that whole-cell platforms for the recombination of cofactors and proteins could be an alternative approach to accelerate the high-throughput screening of ArMs by eliminating the need for in vitro reconstitution steps. One way to overcome these hurdles is to transport the protein to the outer membrane or the periplasm of *E. coli* by tagging the proteins for transport from the cytoplasm and making the protein accessible to the cofactor and assembly in vivo (Figure 1, b).^[9] In addition to these approaches, transferring the cofactor into the cytoplasm is the alternative strategy to realize the construction and reactions of ArMs in whole cells (Figure 1, c).^[10] Recently, coexpression of transporters, such as ChuA and the Hug system, has been used to incorporate cofactors into heme proteins, resulting in a whole-cell catalyst for abiotic reactions and unnatural biosynthesis.^[11] Chiral amines, one of the most important motifs in biomolecules and drugs, have been targets for catalytic processes for many years. Biocatalysis has become an approach for the enantioselective synthesis of chiral amines by transamination or reduction of imines.^[12] In addition to these natural processes, repurposed hemoproteins and ArMs have generated chiral amines by nitrene insertion into C-H bond^[13] and carbene insertions into N-H bonds.^[14] Although high enantioselectivity has been achieved from carbene insertions into Si-H and B-H bonds catalyzed by engineered heme proteins, related enzymatic, enantioselective insertions of carbenes into N-H bonds is limited to specific, cyclic diazo compounds or primary arylamines.^[15] This limitation results from the multi-step pathway that generates a ylide by the attack of the amine and the need for this ylide to undergo proton transfer when bound to the metal or after dissociation from the metal, but before dissociation from the enzyme binding site, if the process is to be enantioselective, design or evolution of an enzyme that catalyzes such enantioselective processes, particularly for alkyl-substituted amines, has been challenging.

We report the application of a whole-cell platform to the directed evolution of ArMs for the catalytic synthesis of chiral amines by enantioselective insertion of an acyclic carbene into the N-H bond of *N*-alkyl arylamines. The whole-cell system, comprising an iridium-containing heme analog, a heme transporter system and coexpressed mutants of the host protein CYP119, was used directly as the catalyst to screen thousands of colonies without cell lysis or protein purification to identify a mutant that catalyzes the synthesis of *N*-methyl amino esters with good enantioselectivity and high turnover numbers (TON) by the reaction of carbene and amine classes that couple with low enantioselectivity when catalyzed by mutants of natural hemoproteins. The enzyme reacts with much higher turnover numbers than chemocatalytic systems to form the tertiary amine ester with comparable enantioselectivity.^[16]

Results and Discussion

Enantioselective carbene insertion into the N-H bond of N-methyl anilines catalyzed by ArMs containing a synthetic Ir-porphyrin cofactor.

Previously, we reported insertions of nitrenes into C-H bonds to form chiral amines catalyzed by ArMs generated by reconstitution of mutants of CYP119, a P450 from the thermophile *Sulfolobus solfataricus* with the artificial cofactor Ir(Me)MPIX, containing the iridium-methyl fragment in mesoporphyrin IX.^[17] With this class of enzyme (Ir-CYP119) we sought to assess the potential of forming chiral amines by carbene insertions into the N-H bonds of amines catalyzed by Ir-CYP119. Tetraarylporphyrin complexes of the Ir-Me unit are known to insert carbenes into the N-H bonds of arylamines,^[18] and the reaction of aniline with ethyl 2-diazopropanoate (Me-EDA) catalyzed by the free Ir(Me)MPIX cofactor formed the chiral amine in good yield and high TON. Encouraged by the high reactivity of the cofactor alone, we sought to use the combination of this cofactor and mutants of the host protein CYP119 to form the chiral amine enantioselectively, while maintaining the high reactivity of the Ir(Me)MPIX unit.

Following previously reported protocols^[19] a preliminary library containing 12 variants of Ir-CYP119 was generated and tested with a series of aniline derivatives. While the insertion process catalyzed by all 12 variants occurred in high yields with aniline, all of the reactions gave racemic product (Table 1, entry 1). However, the reaction of *N*-Me aniline catalyzed by the mutant **CNH-0** (155F, 213G, 254L, 317G) formed the chiral amine with a measurable 40:60 er and acceptable yield (Table 1 entry 2). Aniline derivatives containing electron-withdrawing groups on the nitrogen gave little product (Table 1, entries 3–4). Because of this high reactivity and measurable selectivity for the reaction of *N*-methyl aniline and the lack of enantioselectivity from prior work on the insertions of carbenes into the N-H bonds of *N*-alkyl anilines, we sought to develop reactions with this class of arylamine.

To increase the enantioselectivity of the carbene insertions into the N-H bond, we conducted directed evolution of the Ir-CYP119 system. While directed evolution of ArMs has been reported previously,^[7] we sought to use a new approach to this process by conducting the evolution with our ArMs in whole *E. coli* cells. Our first work on the evolution of Ir-CYP119 enzymes was conducted with purified proteins. We later showed that screening of cell lysates was possible and would eliminate the time-consuming purification of CYP119,^[20] but our initial studies on the insertion of the carbene from Me-EDA into the N-H bond of anilines catalyzed by cell lysates treated with the cofactor Ir(Me)MPIX occurred with almost no enantioselectivity, even for the reaction that occurred with measurable enantioselectivity when catalyzed by the purified protein (Table 1, entry 2 vs Table 1, entry 5). We presumed that this low selectivity resulted from the rapid background reactions catalyzed by unbound Ir(Me)MPIX. To minimize the formation of racemic products formed from the free cofactor, we sought to conduct this directed evolution with the holoenzyme assembled in vivo.

Recently, we demonstrated the efficient transport of an iridium-porphyrin complex into *E. coli* by a heterologous transport system to produce ArMs that form unnatural products by the combination of the reaction of the ArMs with natural enzymes in intact *E. coli*.^[11] The heme transport system encoded by the *hug* operon from *Plesiomonas shigelloides*^[21] led to

the efficient assembly of the ArMs. Thus, to accelerate the directed evolution of ArMs for the insertion of carbenes into N-H bonds, we sought to generate mutants of ArMs containing the Ir(Me)MPIX cofactor in *E. coli* expressing this transport system. Indeed, insertion of the carbene from Me-EDA into the N-H bond of *N*-methyl aniline occurred in the presence of whole cells containing the CYP119 mutant **CNH-0** and the hug operon to form the chiral amino ester product with similar selectivity and higher TON than the reactions catalyzed by the same mutant generated from purified protein (Table 1, entry 6)

Several control experiments were consistent with the reaction by the ArMs assembled *in vivo* by active transport of the cofactor. First, the reaction of *N*-Me aniline and Me-EDA catalyzed by the cell lacking the transporter occurred with lower selectivity and reactivity than that catalyzed by the cells containing the transporter (Table 1, entry 7). These data support the assertion that the products of the pHug operon facilitate the transport of the cofactor to enable assembly of the ArMs *in vivo*. Second, less than 5% of the product was formed from the reactions catalyzed by the cells lacking the gene for CYP119, indicating that this host protein is essential for reactivity. Finally, less than 5% of the product was formed from a reaction occurring without addition of the Me-Ir-MPIX cofactor, ruling out formation of the product by the combination of the CYP119 and a natural cellular component or component of the growth medium (Table 1, entries 8–9). Considering that the free cofactor catalyzes the reaction in pure buffer, we propose that the lack of formation of product by the cofactor without CYP119 results from poisoning of the cofactor by cellular components when it is unprotected by the CYP119 protein.

Directed evolution in whole cells of Ir-CYP119 for asymmetric N-H insertion into *N*-Me aniline.

Having demonstrated that the whole cells containing the transporter, host protein, and artificial cofactor catalyzed the reaction of Me-EDA with *N*-Me aniline with measurable enantioselectivity, the activity and selectivity were increased by directed evolution of the Ir-CYP119 in whole cells. The initial library was generated by combinatorial site-saturation mutagenesis of ten positions (69, 87, 208, 210, 152, 155, 254, 256, 282, 353) around the active site that significantly affected selectivity during our previous studies of carbene transfer reactions.^[19] From several thousand colonies, 96 colonies were randomly chosen for sequencing. Between one and three of the ten positions were mutated in each colony, and mutations at all ten positions appeared among the 96 colonies. After screening of 900 colonies, 12 mutants were identified that reacted with comparable or higher selectivity than the parent mutant. After screening of 900 colonies, 12 mutants were identified that reacted with comparable or higher selectivity than the parent mutant. Comparing with the parent mutant, one or more of the six positions (152, 155, 208, 254, 256, 353) have been modified in these 12 mutants, which indicated these positions are hot spots from ten initial positions. Among these 12 mutants, **CNH-1** (152L, 213G, 254A, and 317G) catalyzed insertion of the carbene unit into the N-H bond with the highest enantioselectivity (Scheme 1, run 1).

Encouraged by this ability to screen the activity and selectivity of the ArMs in whole cells, we conducted a second round of evolution focused on the 152/153/155 positions, which are located in the F-G loop and are considered the entrance of the substrate channel.^[22] Slightly

higher enantioselectivity (36.1% ee) was observed for the reaction catalyzed by the new mutant **CNH-2A** (152S, 153N, 213G, 254A, and 317G) identified after conducting whole-cell reactions of 1080 colonies from the library generated by combinatorial site-saturation mutagenesis of three positions (Scheme 1, run 2A). These colonies were tested in less than two weeks, demonstrating that this whole-cell platform is a much faster system for conducting directed evolution than one based on purified proteins.

Following the approach of Focused Rational Iterative Site-specific Mutagenesis (FRISM),^[22] a third round of evolution was conducted. A library was generated by combinatorial site-specific mutagenesis at the positions (208, 254, 256, and 353) that were found to positively affect the enantioselectivity during the first round of directed evolution but were not covered in run 2A. Instead of generating a saturation mutagenesis library at these four sites, we generated a library containing three amino acids of distinct size (A, L, F) at these four sites that were applied at this round of evolution. Screening 160 colonies of the library covering all four of the above positions showed that the mutant **CNH-3A** (152S, 153N, 208F, 213G, 254A, 256F, and 317G) catalyzes the insertion reaction with a further increased 39.3% ee (Scheme 1, run 3A). Based on this increase resulting from the installation of large amino acid residues at the 208 and 256 positions, mutants containing the other large amino acids (F/Y/W) at positions 208 and 256 were evaluated. However, none of these mutants reacted with higher enantioselectivity than that of the mutant **CNH-3A** (152N, 153S, 208F, 213G, 254A, 256F, and 317G). Revisiting the other positions (210, 254, and 353) by the FRISM strategy did not increase the enantioselectivity over that of the parent mutant. Thus, directed evolution along this path was terminated (Scheme 1, run 4A).

To create a new branch on the evolutionary tree, we conducted a round of evolution from a prior mutant **CNH-1** (152L, 213G, 254A and 317G) with a library focused on positions 208, 210, 254, 256, and 353. Mutations at these positions increased enantioselectivity during the first round of directed evolution that was conducted with combinatorial site-specific mutagenesis. Evaluation of 540 colonies from this library led to a slightly higher ee (32.3% ee) when the reaction was catalyzed by the mutant **CNH-2B** (152L, 208F, 213G, 254A, 256F, and 317G) than with the starting mutant (Scheme 1, run 2B). Further exploration of mutants containing large amino acids at the 208 and 256 positions led to a more selective mutant **CNH-3B** (152L, 208F, 213G, 254A, 256Y, 317G) reacting with 39.6% ee (Scheme 1, run 3B). Finally, we found that an additional mutation of 254C (**CNH-4B**) further improved the ee to 42.5% (Scheme 1, run 4B) with over 20,000 TON in whole cells, based on the amount of iridium cofactor added to the cell culture (Table 2, entry1).

The obvious challenge confronting evolution to form mutants that catalyze this carbene insertion with substantial enantioselectivity and the similar selectivities from several lines of evolution suggest that the evolutionary landscape is rugged. We propose that this challenge arises from counteracting effects of amino acid residues during a multi-step process in which several steps and competing pathways can control enantioselectivity. The ability to achieve substantial enantioselectivity in such a system by generation and testing of more than 4000 colonies illustrates the value of generating and testing the ArMs in whole cells.

Having identified mutants that lead to substantial er, we sought to modify the reaction conditions to increase enantioselectivity further, and the next sections show that this mutant reacts under modified conditions with high enantioselectivity and turnover numbers.

Further increase in enantioselectivity and reactivity by varying reaction conditions

With a highly active and enantioselective mutant in hand, we investigated whether the enantioselectivity could be further improved by modifying the conditions under which the reaction is conducted. Considering the advantages of conducting reactions with lyophilized biocatalyst,^[24] we conducted reactions in two different buffers with lyophilized cell pellets

The redissolved lyophilized cell pellets catalyzed the insertion reactions with higher er (75:25 vs 71:29) than those with fresh cells and with a similarly high TON (Table 2 entries 1–2) in M9-N buffer with the same OD. The increase in enantioselectivity from reactions catalyzed by lyophilized cells was attributed to increasing the permeability of the cells to the reagents, as well as reducing cellular components that might interfere with the reaction. The increased permeability to the reagents would increase the rate of the reaction catalyzed by the holoenzyme, thereby shortening the reaction time and reducing background reaction from free cofactor that could be released from the ArMs over the reaction time.

Changing the reaction buffer from the neutral M9-N (pH 7.4) to the slightly acidic NaPi buffer (pH 6) further increased the enantioselectivity, while maintaining high turnover numbers (Table 2, entries 4–5), most likely by precipitating the misfolded ArMs and reducing the background reactions. Finally, we found that the enantioselectivity further increased from 81:19 er to 87:13 er by reducing the concentration of substrates from 10 mM to 5 mM and the EDA from 40 mM to 20 mM. The higher enantioselectivity from the reactions with a lower concentration of Me-EDA suggests that the high concentration of Me-EDA destabilizes the ArMs, thereby generating the free cofactor that reacts to form the racemic product.

Although the er was higher for reactions with lower concentrations of Me-EDA, the turnover number was lower. Inspired by the increase in TON achieved by slow addition of the diazo compound during our previous studies on C-H insertion reactions catalyzed by Ir-CYP119,^[20] we sought to increase the TON of the addition to the N-H bond by the addition of Me-EDA in batches to prevent decomposition of the diazo reagent and retain the concentration of Me-EDA that leads to high enantioselectivity. Consistent with this hypothesis, high reactivity (8569 TON) and high enantioselectivity (91: 9 er) were observed for reactions conducted by the addition of Me-EDA in four batches over 4 h. Given that the substituent of the ester in the diazo reagents has previously influenced enantioselectivity,^[15a] we tested other diazo esters, but the highest er was achieved with the ethyl ester (Scheme S1).

After identifying mutants and reaction conditions that lead to high activity and enantioselectivity for this carbene transfer, we conducted the reactions of Me-EDA with a variety of *N*-Me aniline derivatives catalyzed by ArMs containing the Ir(Me)MPIX cofactor in *E. coli*. These reactions occurred with various aniline derivatives with good to moderate enantioselectivity under mild conditions. Similar to *N*-Me aniline (**1a**, Table 2, entry 6), para-methyl-substituted *N*-Me aniline (scheme3, **1b**) reacted with Me-EDA

to form the insertion product with good enantioselectivity (86:14 er) and high reactivity (5450 TON) with the same mutant (**CHN-4B**), and the *p*-methoxy-substituted *N*-Me aniline (**1e**) also formed the corresponding chiral amino ester with good selectivity (84:16 er) and high reactivity (2716 TON). Even the bulkier *p*-phenyl-substituted *N*-Me aniline (**1i**) also reacted to form the product of N-H insertion (**3i**) with good enantioselectivity (87:13 er) and high reactivity (2008 TON). However, the enantioselectivity and reactivity of *o*-methyl substituted *N*-Me aniline (**1m**) were lower than those with the *m*-methyl-substituted *N*-Me aniline (**1j**) and *p*-methyl-substituted *N*-Me aniline (**1b**), indicating the steric effects are more pronounced when the substituted group is closer to the reaction center. Moreover, 2-naphthylamine (**1n**), a substrate that reacted with low reactivity during previous studies of enzyme-catalyzed N-H insertion,^[10] reacted readily in *E. coli* containing the ArMs with good TON (2400 TON) and substantial enantioselectivity (76:24 er). Slightly lower selectivity and reactivity were observed for the reaction of Me-EDA with more electron-deficient anilines. For example, the reaction of trifluoromethoxy-substituted **1f** occurred with 69:31 er and 1428 TON, and reactions with *m*-fluoro and trifluoromethyl-substituted anilines (**1k**, **1l**) reacted with lower enantioselectivity (**1k**). Nevertheless, the mild conditions enabled this system to react with good tolerance for functional groups, including a variety of halides (**1c**, **1d**, **1g**) and an ester (**1h**).

Conclusion

We have shown that a whole-cell *E. coli* platform enables directed evolution campaigns with ArMs containing an abiotic Ir-porphyrin cofactor. More than 4000 colonies were generated to develop an enantioselective insertion of an acyclic carbene into the N-H bonds of *N*-methyl anilines, a scope of enantioselective reaction that has evaded prior enzymes generated by mutation of natural P450s. Our assembly of the mutants of ArMs for evolution was enabled by coexpression of the pHug transporter in commercial BL-21(DE) cells. Due to the mild conditions, this transformation accommodates a variety of functional groups. This method for assembling the mutants in whole cells during directed evolution enabled evaluation of much larger mutant libraries than had been possible by testing purified protein and led to products with enantioselectivities closer to those of purified proteins than to those from reactions conducted in cell lysates, which formed product from residual free cofactor. These results show that such whole-cell systems will be valuable for additional directed evolution campaigns aimed at new synthetic transformations.

Supplementary Material

Refer to Web version on PubMed Central for supplementary material.

Acknowledgements

We thank the NIH Institutes of General Medical Sciences (GM-R35130387) for support of this work. Y. G. thanks a joint postdoc fellowship from Pharmaron and Shanghai Institute of Organic Chemistry (SIOC). Z. L. thanks to the National Science Scholarship from the Singapore Agency for Science, Technology and Research.

References

- [1]. Devine PN, Howard RM, Kumar R, Thompson MP, Truppo MD, Turner NJ, *Nat. Rev. Chem* 2018, 2, 409–421
- [2]. Savile CK, Janey JM, Mundorff EC, Moore JC, Tam S, Jarvis WR, Colbeck JC, Krebber A, Fleitz FJ, Brands J, Devine PN, Huisman GW, Hughes GJ, *Science* 2010, 329, 305–309 [PubMed: 20558668]
- [3]. Chen K, Arnold FH, *Nat. Catal* 2020, 3, 203–213.
- [4]. a)Heinisch T, Ward TR, *Acc. Chem. Res* 2016, 49, 1711; [PubMed: 27529561] b)Roelfes G, *Acc. Chem. Res* 2019, 52, 545–556. [PubMed: 30794372]
- [5]. Lewis JC, *Curr. Opin. Chem. Biol* 2015, 25, 27. [PubMed: 25545848]
- [6]. Natoli SN, Hartwig JF, *Acc. Chem. Res* 2019, 52, 326–335 [PubMed: 30693758]
- [7]. Markel U, Sauer DF, Schiffels J, Okuda J, Schwaneberg U, *Angew. Chem. Int. Ed* 2019, 58, 4454–4464
- [8]. Mallin H, Hesticová M, Reuter R, Ward TR, *Nat. Protoc* 2016, 11, 835–852. [PubMed: 27031496]
- [9]. a)Heinisch T, Schwizer F, Garabedian B, Csibra E, Jeschek M, Vallapurackal J, Pinheiro VB, Marlière P, Panke S, Ward TR, *Chem. Sci* 2018, 9, 5383–5388; [PubMed: 30079176] b)Jeschek M, Reuter R, Heinisch T, Trindler C, Klehr J, Panske S, T. R. Ward *Nature* 2016, 537, 661–665; c)Grimm AR, Sauer DF, Polen T, Zhu L, Hayashi T, Okuda J, Schwaneberg U, *ACS Catal.* 2018, 8, 2611–2614.
- [10]. a)Winter MB, McLaurin EJ, Reece SY, Olea C, Nocera DG, Marletta MA, *J. Am. Chem. Soc* 2010, 132, 5582–5583; [PubMed: 20373741] b)Lelyveld VS, Brustad E, Arnold FH, Jasanoff A, *J. Am. Chem. Soc* 2011, 133, 649–651; [PubMed: 21171606] c)Bordeaux M, Singh R, Fasan R, *Bioorg. Med. Chem* 2014, 22, 5697–5704; [PubMed: 24890656] d)Chordia S, Narasimhan S, Paioni AL, Baldus M, Roelfes G, *Angew. Chem. Int. Ed* 2021, 60, 5913–5920.
- [11]. Huang J, Liu Z, Bloomer B, Clark D, Mukhopadhyay A, Keasling J, Hartwig J, *Nat. Chem* 2021, 10.1038/s41557-021-00801-3
- [12]. Ghislieri D, Turner NJ, *Top. Catal* 2014, 57, 284–300.
- [13]. a)Hyster TK, Farwell CC, Buller AR, McIntosh JA, Arnold FH, *J. Am. Chem. Soc* 2014, 136, 15505–15508; [PubMed: 25325618] b)Prier CK, Zhang RJK, Buller AR, Brinkmann-Chen S, Arnold FH, *Nat. Chem* 2017, 9, 629–634; [PubMed: 28644476] c)Yang, Cho I, Qi X, Liu P, Arnold FH, *Nat. Chem* 2019, 11, 987–993. [PubMed: 31611634]
- [14]. a)Wang ZJ, Peck NE, Renata H, Arnold FH, *Chem. Sci* 2014, 5, 598–601; [PubMed: 24490022] b)Sreenilayam G, Fasan R, *Chem. Commun* 2015, 51, 1532–1534.
- [15]. a)Steck V, Carminati DM, Johnson NR, Fasan R, *ACS Catalysis* 2020, 10, 10967–10977; [PubMed: 34484852] b)Liu Z, Calvó-Tusell C, Zhou AZ, Kai C, Garcia-Borràs M, Arnold FH, *Nat. Chem* 2021, 10.1038/s41557-021-00794-z
- [16]. Zhu Y, Liu X, Dong S, Zhou Y, Li W, Lin L, Feng X, *Angew. Chem. Int. Ed* 2014, 53, 1636–1640.
- [17]. Dydio P, Key HM, Hayashi H, Clark DS, Hartwig JF, *J. Am. Chem. Soc* 2017, 139, 1750–1753. [PubMed: 28080030]
- [18]. Anding BJ, Woo LK, *Organometallics* 2013, 32, 2599–2607.
- [19]. Dydio P, Key HM, Nazarenko A, Rha JYE, Seyedkazemi V, Clark DS, Hartwig JF, *Science* 2016, 354, 102–106. [PubMed: 27846500]
- [20]. Gu Y, Natoli SN, Liu Z, Clark DS, Hartwig JF, *Angew. Chem. Int. Ed* 2019, 58, 13954–13960.
- [21]. Smith BJZ, Gutierrez P, Guerrero E, Brewer CJ, Henderson DP, *Appl. Environ. Microbiol* 2011, 77, 6703–6705. [PubMed: 21803893]
- [22]. Basudhar D, Madrona Y, Kandel S, Lampe JN, Nishida CR, de Montellano PRO, *J. Biol. Chem* 2015, 290, 10000–10017. [PubMed: 25670859]
- [23]. Li D, Wu Q, Reetz MT, *Methods Enzymol.* 2020, 643, 225–242. [PubMed: 32896283]
- [24]. Montañez-Clemente I, Alvira E, Macias M, Ferrer A, Fonceca M, Rodriguez J, Rodriguez J, Gonzalez A, Barletta G, *Biotechnol. Bioeng* 2002, 78, 53–59. [PubMed: 11857281]

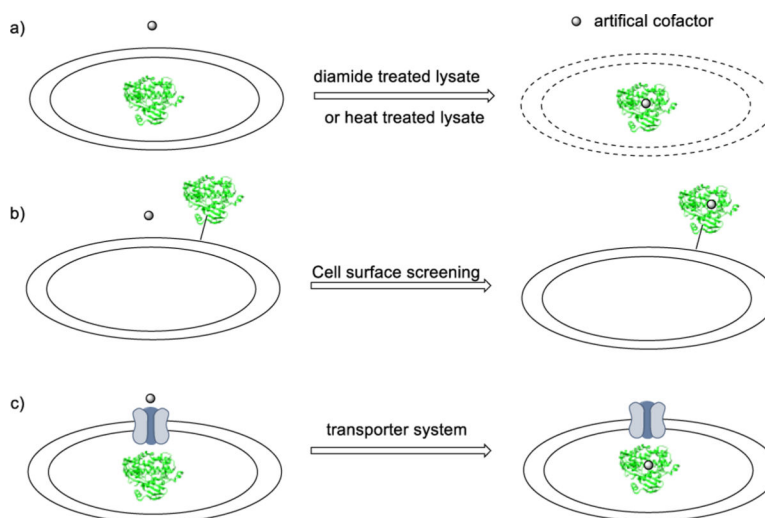


Figure 1. Approaches to assemble ArMs during a directed evolution campaign. (a) Screening in cell lysates with an additional step to remove nonspecific conjugation; (b) screening in vivo by cell surface display, and (c) in vivo assembly of Ir-CYP119 with a system to transport the cofactor into the cytoplasm.

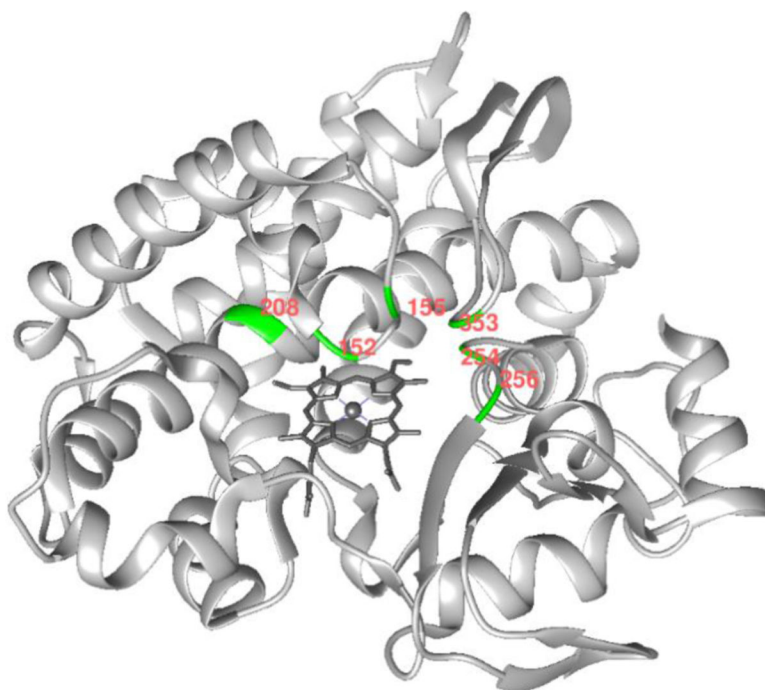
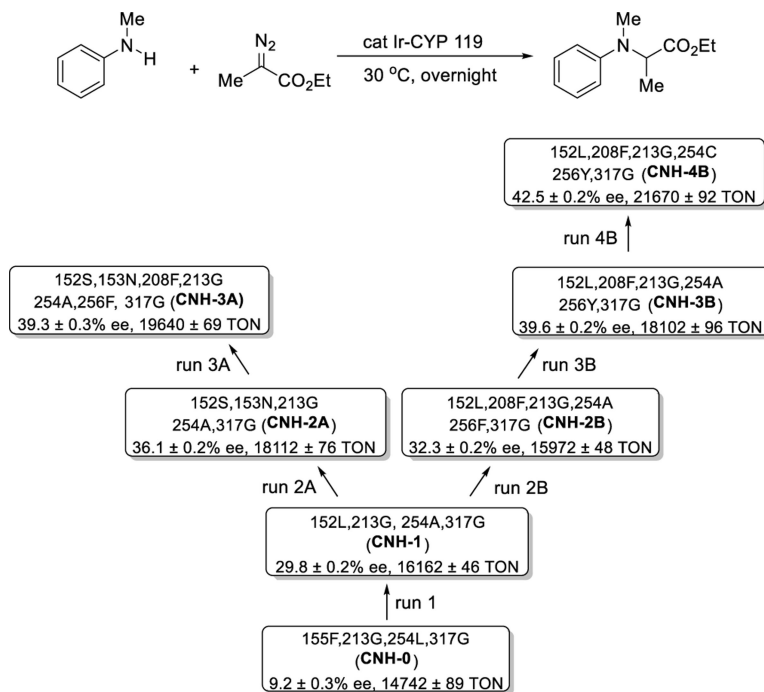
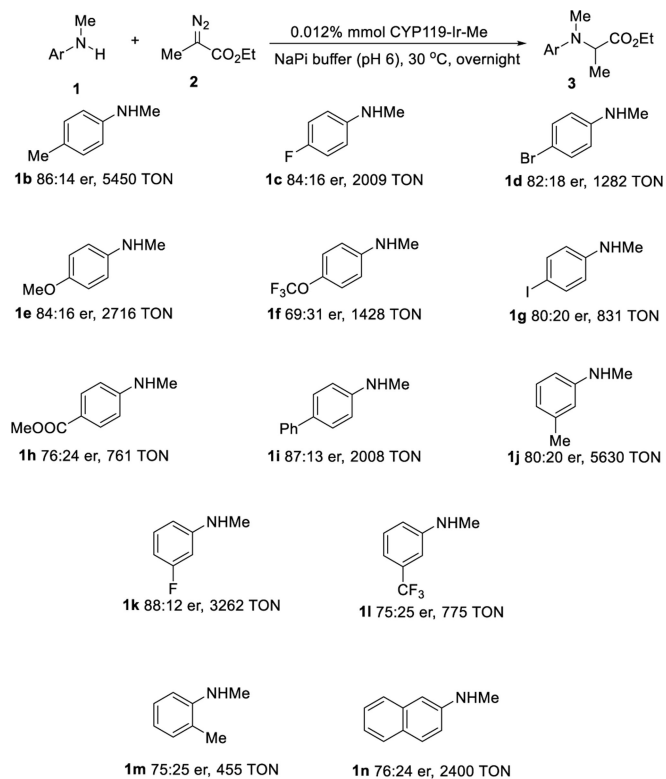


Figure 2. Structure of wild-type Fe-CYP119 (image prepared in Chimera from PDB **1IO7**). The positions modified during the directed evolution are highlighted in green with red labels.

**Scheme 1.**

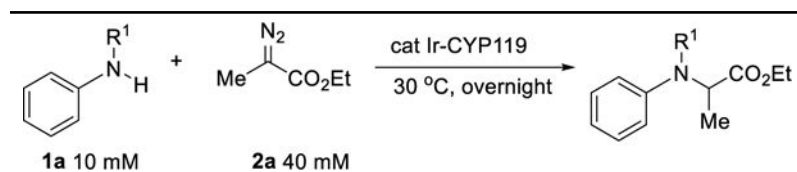
Directed evolution of carbene insertion into the N-H bond by screening of whole-cells^{a,b}

a) Reaction conditions: BL-21(DE) coexpressing the CYP119 mutants and hug operon, $OD_{600} \sim 25$, 0.0025 % mol Ir(Me)-MPIX, *N*-Me aniline (2.5 μ mol), EDA (10 μ mol), DMSO (10 μ L), M9-N (250 μ L), 30 °C, overnight. b) The ee was determined by chiral HPLC and was the average of three reactions; The TON was calculated by the number of substrate molecules converted to the product per iridium cofactor added to the cell culture and was the average of three reactions; ee was used instead of er in this scheme as the measure of enantioselectivity to show more clearly the experimental error in the selectivities.

**Scheme 2.**

Scope of carbene insertion catalyzed by ArMs containing Me-Ir-MPIX in the whole cell.^{a,b,c}

a) Reaction conditions: BL-21(DE) coexpressing the CYP119 **CNH-4B** and the hug operon, OD₆₀₀ ~50, 0.01 %mol Ir(Me)-MPIX, *N*-Me aniline derivatives (5 μmol), EDA (20 μmol, addition in four batches over 4 h), DMSO (20 μL), NaPi (1.0 mL), 30 °C, overnight. b) The er was determined by chiral HPLC and was the average of three reactions. c) The TON was calculated by the number of substrate molecules converted to the product per iridium cofactor added to the cell culture and was the average of three reactions.

Table 1.Initial studies of carbene insertion into the N-H bond of *N*-Me aniline catalyzed by (Me)IrCYP119.^a

entry	R ¹	Catalyst	er ^b	Yield ^b	TON ^c
1	H	Purified ArM	50:50	92%	1840
2	Me	Purified ArM	40:60	56%	1120
3	Ac	Purified ArM	ND	<5%	--
4	Ts	Purified ArM	ND	<5%	--
5	Me	Cell lysis ArM	50:50	54%	1080
6 ^d	Me	whole cell	39:61	59%	5867
7 ^e	Me	whole cell	45:55	23%	2257
8 ^f	Me	whole cell	ND	<5%	--
9 ^g	Me	whole cell	ND	<5%	--

^a) Reaction conditions: 2.5 μmol aniline derivatives, 10 μmol Me-EDA, 0.05 mol% Ir(Me)-MPIX with the **CNH-0** mutant (155F, 213G, 254L, and 317G), 0.25 mL M9-N buffer, 30 $^\circ\text{C}$, overnight.

^b) The er and yield were determined by chiral HPLC with *N,N*-diethylaniline as the internal standard.

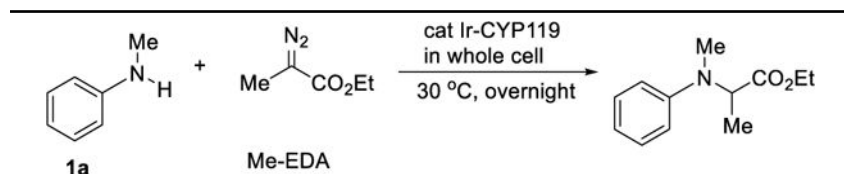
^c) The TON was calculated by the number of substrate molecules converted to the product per iridium cofactor added to the cell culture.

^d) The reactions were run in whole cells at an OD ~ 25 coexpressing the hug operon and CYP119 and 0.01 mol % Ir(Me)-MPIX.were

^e) The reactions run in whole cells with only CYP119 expression.

^f) The reactions run in whole cells with coexpressing the hug operon and a blank 2BT vector.

^g) The reactions were run in whole cells coexpressing the hug operon and CYP119 but without the addition of Ir(Me)MPIX.

Table 2.Evaluation of whole-cell reaction conditions for carbene insertion into the N-H bond of *N*-Me aniline.^{a,b}

entry	1a (mM)	Me-EDA (mM)	reaction buffer	OD	Catalyst	er ^b	TON ^c
1	10	40	M9-N	25	Fresh cell	71:29	21670
2	10	40	M9-N	25	lyophilized cell	75:25	20895
3	10	40	M9-N	50	lyophilized cell	78:22	17867
4	10	40	NaPi	50	lyophilized cell	81:19	14536
5	5	20	NaPi	50	lyophilized cell	87:13	3210
6 ^d	5	20	NaPi	50	lyophilized cell	91:9	8569

^{a)} Reaction conditions: BL-21(DE) coexpressing the hug operon and the CYP119 mutant **CNH-4B**, 0.0025 mol % to 0.01 mol % Ir(Me)-MPIX based on the OD, 30 °C, 4 h.

^{b)} The er was determined by chiral HPLC and was the average of three reactions.

^{c)} The TON was calculated by the number of substrate molecules converted to the product per iridium cofactor added to the cell culture and was the average of three reactions.

^{d)} The reaction was performed with the addition of Me-EDA in four batches over 4 h.